LA-UR-02-1920
Approved for public release;
distribution is unlimited.

Title: **QCD Coherence Effects in High Energy Reactions with Nuclei**

Author(s): Jörg Raufeisen

Submitted to:

http://lib-www.lanl.gov/cgi-bin/getfile?00818823.pdf

QCD Coherence Effects in High Energy Reactions with Nuclei

Jörg Raufeisen
Los Alamos National Laboratory, MS H846,
Los Alamos, NM 87545, USA

ABSTRACT

We investigate QCD coherence effects in deep inelastic scattering (DIS) off nuclei and in Drell-Yan (DY) dilepton production in proton-nucleus collisions within the light-cone color-dipole approach. The physical mechanisms underlying the nuclear effects become very transparent in this approach and are explained in some detail. We present numerical calculations of nuclear shadowing in DIS and DY and compare to data. Nuclear effects in the DY transverse momentum distribution are calculated as well. The dipole approach is the only known way to calculate the Cronin effect without introducing additional parameters for nuclear targets.

Keywords: Deep Inelastic Scattering, Drell-Yan Process, QCD, Nuclear Effects, Coherence Effects, Multiple Scattering.

1. INTRODUCTION

The use of nuclei instead of protons in high energy scattering experiments, like deep inelastic scattering, provides unique possibilities to study the space-time development of strongly interacting systems. In experiments with proton targets the products of the scattering process can only be observed in a detector which is separated from the reaction point by a macroscopic distance. In contrast to this, the nuclear medium can serve as a detector located directly at the place where the microscopic interaction happens. As a consequence, with nuclei one can study coherence effects in QCD which are not accessible in DIS off protons nor in proton-proton scattering.

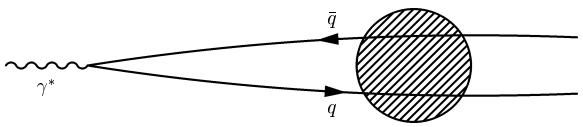

FIG. 1: At low x_{Bj} and in the target rest frame, the virtual photon γ^* converts into a $q\bar{q}$-pair long before the target.

At high energies, nuclear scattering is governed by coherence effects which are most easily understood in the target rest frame. In the rest frame, DIS looks like pair creation from a virtual photon, see Fig. 1. Long before the target, the virtual photon splits into a $q\bar{q}$-pair. The lifetime l_c of the fluctuation, which is also called coherence length, can be estimated with help of the uncertainty relation to be of order $\sim 1/m_N x_{Bj}$, where x_{Bj} is Bjorken-x and $m_N \approx 1$ GeV is the nucleon mass. The coherence length can become much greater than the nuclear radius at low x_{Bj}. Multiple scattering within the lifetime of the $q\bar{q}$ fluctuation leads to the pronounced coherence effects observed in experiment.

The most prominent example for a coherent interaction of more than one nucleon is the phenomenon of nuclear shadowing, *i.e.* the suppression of the nuclear structure function F_2^A with respect to the proton structure function F_2^p at low $x_{Bj} \lesssim 0.1$, $F_2^A(x_{Bj},Q^2)/(AF_2^p(x_{Bj},Q^2))$. Here Q^2 is the virtuality of the photon. Shadowing in low x_{Bj} DIS and at high photon virtualities is experimentally well studied by NMC [1]. The analogous effect for DY at low x_2 was discovered by E772 [2].

What is the mechanism behind this suppression? If the coherence length is very long, as indicated in Fig. 1, the $q\bar{q}$-dipole undergoes multiple scatterings inside the nucleus. The physics of shadowing in DIS is most easily understood in a representation, in which the pair has a definite transverse size ρ. As a result of color transparency [3–5], small pairs interact with a small cross section, while large pairs interact with a large cross section. The term "shadowing" can be taken literally in the target rest frame. Large pairs are absorbed by the nucleons at the surface which cast a shadow on the inner nucleons. The small pairs are not shadowed. They have equal chances to interact with any of the nucleons in the nucleus. From these simple arguments, one can already understand the two necessary conditions for shadowing. First, the hadronic fluctuation of the virtual photon has to interact with a large cross section and second, the coherence length has to be long enough to allow for multiple scattering.

While the target rest frame picture of DIS is very popular, the light-cone approach of Kopeliovich [6–8], which describes the DY process [9] in the target rest frame, is less known. In the light-cone approach, DY dilepton production in the rest frame of the target appears as bremsstrahlung, see Fig. 2. A quark from the projectile scatters off the target and radiates a virtual photon. This photon decays into a lepton pair. Even

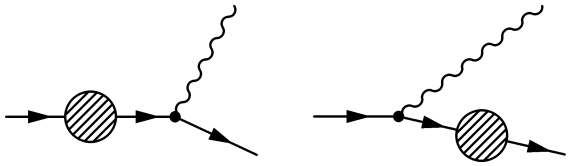

FIG. 2: A quark (or an antiquark) inside the projectile hadron scatters off the target color field and radiates a massive photon. The subsequent decay of the γ^* into the lepton pair is not shown.

though this mechanism looks quite different from the usual annihilation picture, it yields numerical values very similar to the next-to-leading order parton model [11]. Note that while cross sections are Lorentz invariant, the partonic interpretation of a hard scattering process is not. That is why a process that looks like quark-antiquark annihilation in the infinite momentum frame can appear as bremsstrahlung in the target rest frame.

Remarkably, the DY cross section can be expressed in terms of the same dipole cross section that appears in DIS. In DY, the dipole cross section arises from the interference of the two graphs in Fig. 2. On a nuclear target, the quark will of course scatter several times. The effect of multiple scattering on bremsstrahlung is well known in QED as the Landau-Pomeranchuk-Migdal (LPM) effect [10]. The LPM effect leads to a reduction of the cross section due to destructive interferences between the amplitudes for radiation off different points along the quark's trajectory. In the case of DY, this suppression is observed in experiment as nuclear shadowing [2].

2. SHADOWING IN DIS

First, we discuss the case of shadowing in deep inelastic scattering off nuclei. Like shadowing in hadron-nucleus collisions [12], also shadowing in DIS is intimately related to diffraction. The close connection between shadowing and diffraction becomes most transparent in the formula derived by Karmanov and Kondratyuk [13]. In the double scattering approximation, the shadowing correction can be related to the diffraction dissociation spectrum, integrated over the mass,

$$\begin{aligned}\sigma^{\gamma^* A} &\approx A\sigma^{\gamma^* p} \\ &- 4\pi \int dM_X^2 \left.\frac{d\sigma(\gamma^* N \to XN)}{dM_X^2\, dt}\right|_{t\to 0} \\ &\times \int d^2b F_A^2(l_c, b). \end{aligned} \tag{1}$$

Here

$$F_A^2(l_c, b) = \left| \int_{-\infty}^{\infty} dz \rho_A(b,z) \mathrm{e}^{\mathrm{i}z/l_c} \right|^2 \tag{2}$$

is the formfactor of the nucleus, which depends on the coherence length

$$l_c = \frac{2\nu}{Q^2 + M_X^2}, \tag{3}$$

ν is the energy of the γ^* in the target rest frame and M_X is the mass of the diffractively excited state. The coherence length can be estimated from the uncertainty relation and is the lifetime of the diffractively excited state. If $l_c \to 0$, the shadowing correction in Eq. (1) vanishes and one is left with the single scattering term $A\sigma^{\gamma^* p}$.

Note that Eq. (1) is valid only in double scattering approximation. For heavy nuclei, however, higher order scattering terms will become important. These can be calculated, if one knows the eigenstates of the interaction. Fortunately, the eigenstates of the T matrix (restricted to diffractive processes) were identified a long time ago in QCD [3, 14] as partonic configurations with fixed transverse separations in impact parameter space. For DIS, the lowest eigenstate is the $q\bar{q}$ Fock component of the photon. The total γ^*-proton cross section is easily calculated, if one knows the cross section $\sigma_{q\bar{q}}(\rho)$ for scattering a $q\bar{q}$-dipole of transverse size ρ off a proton,

$$\sigma^{\gamma^* p} = \int d\alpha d^2\rho \left|\Psi_{q\bar{q}}(\alpha,\rho)\right|^2 \sigma_{q\bar{q}}(\rho). \tag{4}$$

The light-cone wavefunction $\Psi_{q\bar{q}}(\alpha,\rho)$ describes the splitting of the virtual photon into the $q\bar{q}$-pair and is calculable in perturbation theory, see *e.g.* [15]. Here, α is the longitudinal momentum fraction carried by the quark in Fig. 1. The dipole cross section is governed by nonperturbative effects and cannot be calculated from first principles. We use the phenomenological parameterization from [16] for our calculation of shadowing in DIS, which is fitted to HERA data on the proton structure function. Note that higher Fock-states of the photon, containing gluons, lead to an energy dependence of $\sigma_{q\bar{q}}$, which we do not write out explicitly.

The diffractive cross section can also be expressed in terms of $\sigma_{q\bar{q}}$. Since the cross section for diffraction is proportional to the square of the T-matrix element, $|\langle\gamma^*|T|X\rangle|^2$, the dipole cross section also enters squared,

$$\int dM_X^2 \left.\frac{d\sigma(\gamma^* N \to XN)}{dM_X^2\, dt}\right|_{t\to 0} = \frac{\langle\sigma_{q\bar{q}}^2(\rho)\rangle}{16\pi}, \tag{5}$$

where the brackets $\langle\ldots\rangle$ indicate averaging over the light-cone wavefunctions like in Eq. (4). We point out

that in order to reproduce the correct behavior of the diffractive cross section at large M_X, one has to include at least the $q\bar{q}G$ Fock-state of the γ^*. This correction is, however, of minor importance in the region where shadowing data are available.

If one attempts to calculate shadowing from Eq. (1) with help of Eq. (5), one faces the problem that the nuclear form factor, Eq. (2), depends on the mass M_X of the diffractively produced state, which is undefined in impact parameter representation. Only in the limit $l_c \gg R_A$, where R_A is the nuclear radius, it is possible to resum the entire multiple scattering series in an eikonal-formula

$$\sigma^{\gamma^* A} = \left\langle 2 \int d^2b \left(1 - \exp\left(-\frac{\sigma_{q\bar{q}}(\rho)}{2} T(b) \right) \right) \right\rangle . \quad (6)$$

The nuclear thickness function $T(b) = \int_{-\infty}^{\infty} dz\, \rho_A(b,z)$ is the integral of nuclear density over longitudinal coordinate z and depends on the impact parameter b. The condition $l_c \gg R_A$ insures that the ρ does not vary during propagation through the nucleus (Lorentz time dilation) and one can apply the eikonal approximation.

The condition $l_c \gg R_A$ is however not fulfilled in experiment. For the case $l_c \sim R_A$, one has to take the variation of ρ during propagation of the $q\bar{q}$ fluctuation through the nucleus into account, see Fig. 3. A widely used recipe is to replace $M_X^2 \to Q^2$, so that $l_c \to 1/(2m_N x_{Bj})$ and one can apply the double scattering approximation. This recipe was, however, disfavored during our investigation [17]. Moreover, there is no simple recipe to include a finite l_c into higher order scattering terms.

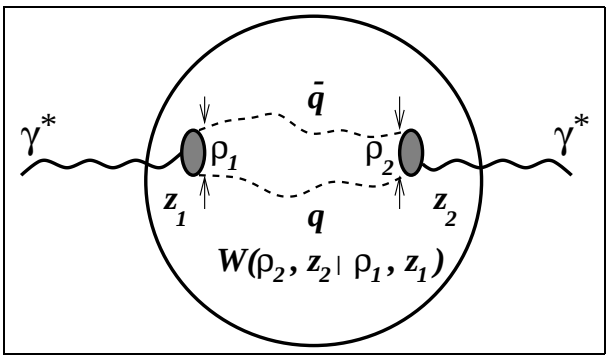

FIG. 3: Propagation of a $q\bar{q}$-pair through a nucleus. Shown is the case of a finite coherence length, where the transverse motion is described by the Green function $W(\vec{\rho}_2, z_2|\vec{\rho}_1, z_1)$.

In [18] a Green function technique was developed that provides the correct quantum-mechanical treatment of a finite coherence length in all multiple scattering terms. Like in Eq. (1) the total cross section is represented in the form

$$\sigma^{\gamma^* A} = A\sigma^{\gamma^* p} - \Delta\sigma, \quad (7)$$

where $\Delta\sigma$ is the shadowing correction,

$$\begin{aligned} \Delta\sigma &= \frac{1}{2}\mathrm{Re} \int d^2b \int_{-\infty}^{\infty} dz_1 \rho_A(b,z_1) \int_{z_1}^{\infty} dz_2 \rho_A(b,z_2) \\ &\times \int_0^1 d\alpha \int d^2\rho_2 \Psi^*_{q\bar{q}}(\vec{\rho}_2,\alpha)\sigma_{q\bar{q}}(\rho_2) \\ &\times A(\vec{\rho}_2, z_1, z_2, \alpha), \end{aligned} \quad (8)$$

with

$$\begin{aligned} A(\vec{\rho}_2, z_1, z_2, \alpha) &= \int d^2\rho_1\, W(\vec{\rho}_2, z_2|\vec{\rho}_1, z_1) \\ &\times \mathrm{e}^{-\mathrm{i}q_L^{min}(z_2-z_1)}\, \sigma_{q\bar{q}}(\rho_1)\, \Psi_{q\bar{q}}(\vec{\rho}_1,\alpha). \end{aligned} \quad (9)$$

Here,

$$q_L^{min} = \frac{1}{l_c^{max}} = \frac{Q^2\alpha(1-\alpha) + m_f^2}{2\nu\alpha(1-\alpha)} \quad (10)$$

is the minimal longitudinal momentum transfer when the photon splits into the $q\bar{q}$ dipole (m_f is the quark mass).

The shadowing term in Eq. (7) is illustrated in Fig. 3. At the point z_1 the photon diffractively produces the $q\bar{q}$ pair ($\gamma^* N \to q\bar{q}N$) with a transverse separation $\vec{\rho}_1$. The pair propagates through the nucleus along arbitrarily curved trajectories, which are summed over, and arrives at the point z_2 with a separation $\vec{\rho}_2$. The initial and the final separations are controlled by the light-cone wavefunction $\Psi_{q\bar{q}}(\vec{\rho},\alpha)$. While passing the nucleus the $q\bar{q}$ pair interacts with bound nucleons via the cross section $\sigma_{q\bar{q}}(\rho)$ which depends on the local separation $\vec{\rho}$. The Green function $W(\vec{\rho}_2, z_2|\vec{\rho}_1, z_1)$ describes the propagation of the pair from z_1 to z_2, see Eq. (9), including all multiple rescatterings and a finite coherence length. Note the diffraction dissociation (DD) amplitude,

$$f_{DD}(\gamma^* \to q\bar{q}) = \mathrm{i}\Psi_{q\bar{q}}(\vec{\rho}_1,\alpha)\sigma_{q\bar{q}}(\rho_1) \quad (11)$$

, in Eq. (9). At the position z_2, the result of the propagation is again projected onto the diffraction dissociation amplitude, Eq. (8). The Green function includes that part of the phase shift between the initial and the final photons which is due to transverse motion of the quarks, while the longitudinal motion is included in Eq. (9) via the exponential.

The Green function $W(\vec{\rho}_2, z_2; \vec{\rho}_1, z_1)$ in Eq. (9) satisfies the two dimensional Schrödinger equation,

$$\begin{aligned} \mathrm{i}\frac{\partial W(\vec{\rho}_2, z_2|\vec{\rho}_1, z_1)}{\partial z_2} &= \\ &- \frac{\Delta(\rho_2)}{2\nu\alpha(1-\alpha)} W(\vec{\rho}_2, z_2|\vec{\rho}_1, z_1) \\ &- \frac{\mathrm{i}}{2}\sigma(\rho_2)\rho_A(b,z_2) W(\vec{\rho}_2, z_2|\vec{\rho}_1, z_1) \end{aligned} \quad (12)$$

with the boundary condition $W(\vec{\rho}_2, z_1|\vec{\rho}_1, z_1) = \delta^{(2)}(\vec{\rho}_2 - \vec{\rho}_1)$. The Laplacian $\Delta(\rho_2)$ acts on the coordinate $\vec{\rho}_2$. The kinetic term $\Delta/[2\nu\alpha(1-\alpha)]$ in this Schrödinger equation takes care of the varying effective mass of the $q\bar{q}$ pair and provides the proper phase shift. The role of time is played by the longitudinal coordinate z_2. The imaginary part of the optical potential describes the rescattering.

The Green function method contains the eikonal approximation Eq. (6) and the Karmanov-Kondratyuk formula Eq. (1) as limiting cases. In order to obtain the eikonal approximation, one has to take the limit $\nu \to \infty$. In this case, the kinetic energy term in Eq. (12) can be neglected and with $q_L^{min} \to 0$ one arrives after a short calculation at Eq. (6).

One can also recover the Karmanov-Kondratyuk formula, when one neglects the imaginary potential in Eq. (12). Then W becomes the Green function of a free motion.

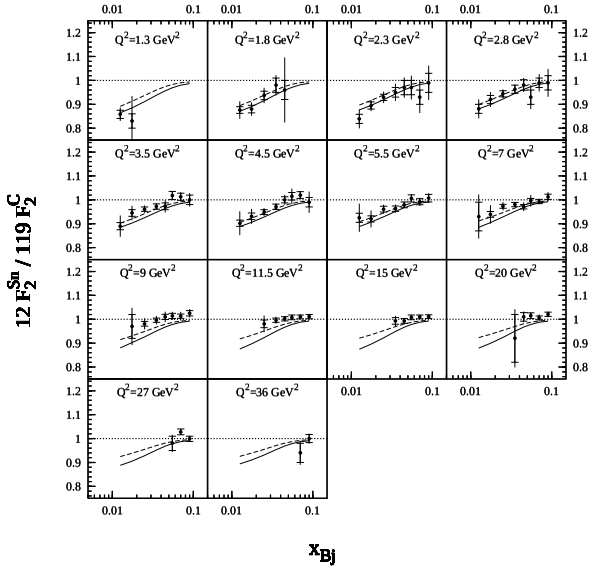

FIG. 4: The x_{Bj} dependence of shadowing in DIS for the structure function of tin relative to carbon. The data are from NMC [1]. The full curves are calculated in the Green-function approach, including the nonperturbative interaction between the q and the $\bar{q}$. The dashed curve does not include this interaction. The figure is from [16].

Calculations in the Green function approach are compared to NMC data in Fig. 4. Note that the leading twist contribution to shadowing is due to large dipole sizes, where nonperturbative effects, like an interaction between the q and the $\bar{q}$, might become important. Therefore, the solid curve is calculated following [19], including such an interaction. This interaction modifies the light-cone wavefunction [19]. The dashed curve is calculated with the conventional, perturbative light-cone wavefunctions, but including a constituent quark mass. Both curves are in reasonable agreement with the data.

Note that for these data, the coherence length is of order of the nuclear radius or smaller. Indeed, shadowing vanishes around $x_{Bj} \approx 0.1$, because the coherence length becomes smaller than the mean internucleon spacing. Therefore, the eikonal approximation, Eq. (6), cannot be applied for the kinematics of NMC and a correct treatment of the coherence length becomes crucial. We emphasize that the calculation in Fig. 4 does not contain any free parameters. Following the spirit of Glauber theory, all free parameters are adjusted to DIS off protons.

3. NUCLEAR EFFECTS IN THE DRELL-YAN PROCESS

In the second part of this paper, we discuss the application of the dipole approach to calculate nuclear effects in DY. The main features of the approach have already been introduced in the preceding section and the case of DY is almost completely analogous to DIS.

The cross section for radiation of a virtual photon from a quark after scattering on a proton, can be written in factorized light-cone form [6–8],

$$\frac{d\sigma(qp \to \gamma^* X)}{d\ln\alpha} = \int d^2\rho\, |\Psi_{\gamma^* q}(\alpha,\rho)|^2 \sigma_{q\bar{q}}(\alpha\rho), \quad (13)$$

with the same $\sigma_{q\bar{q}}$ as in DIS. Again, the light-cone wavefunction $\Psi_{\gamma^* q}(\alpha,\rho)$ is calculable in perturbation theory [11, 20]. For DY, however, ρ is the photon-quark transverse separation and α is the fraction of the light-cone momentum of the initial quark taken away by the photon. We use the standard notation for the kinematical variables, $x_1 - x_2 = x_F$, $\tau = M^2/s = x_1 x_2$, where x_F is the Feynman variable, s is the center of mass energy squared of the colliding protons and M is the dilepton mass.

The physical interpretation of (13) is similar to the DIS case. Long before the target, the projectile quark develops fluctuations which contain virtual photons. On interaction with the target, these fluctuations can be put on mass shell and the γ^* is freed. In order to make this happen, the interaction must distinguish between Fock states with and without γ^*, *i.e.* these states have to interact differently. Since only the quark interacts in both Fock components, the difference in the scattering amplitudes arises from the relative displacement of the quark in the transverse plane when it radiates a photon. The $\gamma^* q$ fluctuation has a center of gravity in the transverse plane which coincides with the impact parameter of the parent quark. One finds that the transverse separation between the quark and the center of gravity is $\alpha\rho$, *i.e.* the argument of $\sigma_{q\bar{q}}$. The dipole cross section arises from the interference of the two graphs in Fig. 2 and should

be interpreted as freeing cross section for the virtual photon. More discussion can be found in [20].

The transverse momentum distribution of DY pairs can also be expressed in terms of the dipole cross section [8]. The differential cross section is given by the Fourier integral

$$\begin{aligned}\frac{d\sigma(qp\to\gamma^* X)}{d\ln\alpha d^2q_T} &= \\ &= \frac{1}{(2\pi)^2}\int d^2\rho_1 d^2\rho_2\,\exp[\mathrm{i}\vec{q}_T\cdot(\vec{\rho}_1-\vec{\rho}_2)] \\ &\times\ \Psi^*_{\gamma^* q}(\alpha,\vec{\rho}_1)\Psi_{\gamma^* q}(\alpha,\vec{\rho}_2) \qquad (14)\\ &\times\ \frac{1}{2}\left\{\sigma_{q\bar{q}}(\alpha\rho_1)+\sigma_{q\bar{q}}(\alpha\rho_2)-\sigma_{q\bar{q}}(\alpha(\vec{\rho}_1-\vec{\rho}_2))\right\}.\end{aligned}$$

After integrating this expression over the transverse momentum q_T of the photon, one obviously recovers Eq. (13).

Nuclear effects arise in the DY process, because the different nucleons in the nucleus compete to free the γ^*. Necessary condition for this phenomenon is of course that the coherence length for DY,

$$l_c = \frac{1}{m_N x_2}\frac{(1-\alpha)M^2}{q_T^2+(1-\alpha)M^2+\alpha^2 m_f^2} \qquad (15)$$

exceeds the mean internucleon spacing of ~ 2 fm. At infinite coherence length, one can simply eikonalize the dipole cross section, similar to the DIS case, cmp. Eq. (6). For finite coherence length, the Green function technique can be developed for DY in complete analogy to DIS. We do not display the corresponding formula here, which can be found in [8, 16, 21]. We point out that even though DIS and DY appear very similar in the dipole approach, there are no (or only very few) diffractively produced DY pairs, because Eq. (5) is not applicable to an exclusive channel (see discussion in [19]).

Calculations of shadowing for DY in the Green function approach are compared to E772 data [2] in Fig. 5. Like in the case of the NMC data in the previous section, the coherence length l_c at E772 energy becomes smaller than the nuclear radius. Shadowing vanishes as x_2 approaches 0.1, because the coherence length becomes smaller than the mean internucleon separation. Again, it is therefore important to have a correct description of a finite l_c. The eikonal approximation does not reproduce the vanishing shadowing toward $x_2 \to 0.1$, because it assumes an infinite coherence length.

The curves in Fig. 5 are somewhat different from the ones in [16, 21], because we used a different parameterization of the dipole cross section [22]. Note that for heavy nuclei, energy loss [23] leads to an additional suppression of the DY cross section. It is therefore important to calculate shadowing in DY without introducing additional parameter for nuclear targets.

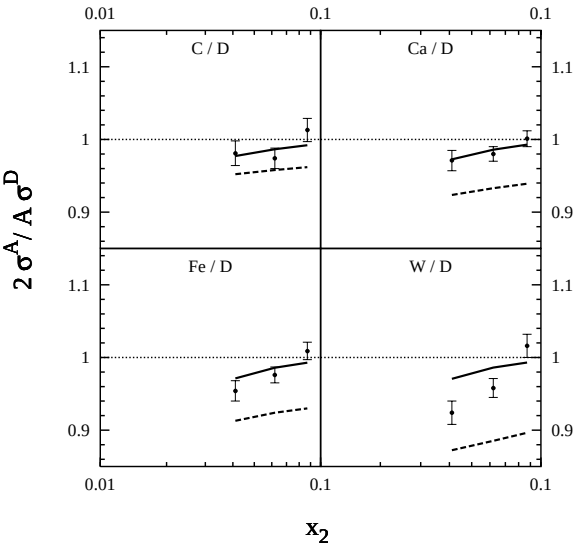

FIG. 5: Comparison between calculations in the Green function technique (solid curve) and E772 data at center of mass energy $\sqrt{s} = 38.8$ GeV for shadowing in DY. The dashed curve shows the eikonal approximation, which is not valid at this energy, any more.

Otherwise, shadowing and energy loss cannot be disentangled.

Nuclear effects on the q_T-differential cross section calculated at RHIC and LHC energy are shown in Fig. 6. At these high *cm* energies, the coherence length significantly exceeds the nuclear radius, justifying the eikonal approximation. However, in the case of such long l_c, the quark has sufficient time to radiate additional gluons. Thus, higher Fock states have to be taken into account. This is accomplished by multiplying $\sigma_{q\bar{q}}$ with the gluon shadowing ratio R_G, which was calculated in [19]. See [24] for a detailed discussion.

The differential cross section is suppressed at small

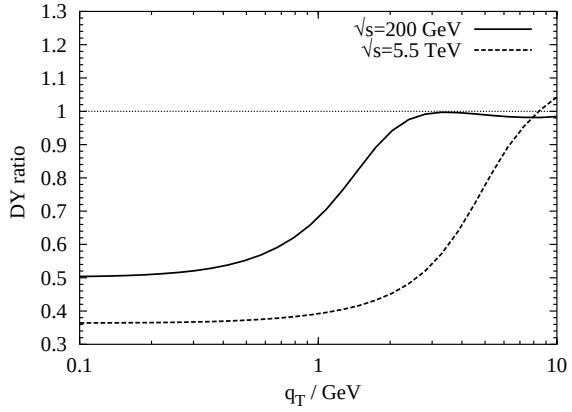

FIG. 6: Nuclear effects on the DY transverse momentum distribution at RHIC and LHC for dilepton mass $M = 4.5$ GeV and Feynman $x_F = 0.5$.

transverse momentum q_T of the dilepton, where large values of ρ dominate. This suppression vanishes at intermediate $q_T \sim 2$ GeV. The Cronin enhancement that one could expect in this intermediate q_T region [21] is suppressed due to gluon shadowing [24]. At very large transverse momentum nuclear effects vanish.

4. SUMMARY

In the target rest frame and at low x_{Bj} (x_2), the cross sections for DIS and DY can both be expressed in terms of the same cross section for scattering a color-neutral $q\bar{q}$-pair off a proton. The advantage of this formulation and the main motivation to develop this approach is the easy generalization to nuclear targets and the insight into the dynamical origin of nuclear effects, which appear as coherence effects due to multiple scattering.

The main nonperturbative input to all formulae is the dipole cross section, which cannot be calculated from first principles. Instead one uses a phenomenological parameterization for this quantity, which is determined to fit DIS data from HERA. Nuclear effects are then calculated without introducing any new parameters. A parameter free calculation of nuclear shadowing for DY is indispensable, if one aims at extracting the energy loss of a fast quark propagating through nuclear from DY data [23]. Furthermore, the dipole formulation is the only known way to calculate the Cronin effect in a parameter free way. This approach can also be applied to calculate the Cronin effect in hadronic collisions [25]. Furthermore, a good description of NMC data on shadowing in DIS is achieved.

Finally, we mention that the dipole approach can also be applied to a variety of other processes, *e.g.* heavy quark, quarkonium or vector meson production [26].

Acknowledgments: This work was supported by the U.S. Department of Energy at Los Alamos National Laboratory under Contract No. W-7405-ENG-38. The author is grateful to Jörg Hüfner, Mikkel Johnson, Boris Kopeliovich, Jen-Chieh Peng and Alexander Tarasov for valuable discussion.

[1] M. Arneodo *et al.* [New Muon Collaboration], Nucl. Phys. B **481**, 23 (1996).
[2] D. M. Alde *et al.*, Phys. Rev. Lett. **64**, 2479 (1990).
[3] A. B. Zamolodchikov, B. Z. Kopeliovich and L. I. Lapidus, JETP Lett. **33**, 595 (1981) [Pisma Zh. Eksp. Teor. Fiz. **33**, 612 (1981)];
[4] G. Bertsch, S. J. Brodsky, A. S. Goldhaber and J. F. Gunion, Phys. Rev. Lett. **47**, 297 (1981).
[5] S. J. Brodsky and A. H. Mueller, Phys. Lett. **206B**, 685 (1988).
[6] B. Z. Kopeliovich, proc. of the workshop Hirschegg '95: Dynamical Properties of Hadrons in Nuclear Matter, Hirschegg January 16-21, 1995, ed. by H. Feldmeyer and W. Nörenberg, Darmstadt, 1995, p. 102 (hep-ph/9609385).
[7] S. J. Brodsky, A. Hebecker and E. Quack, Phys. Rev. D **55**, 2584 (1997).
[8] B. Z. Kopeliovich, A. Schäfer and A. V. Tarasov, Phys. Rev. C **59**, 1609 (1999), extended version in hep-ph/9808378.
[9] S. D. Drell and T. Yan, Phys. Rev. Lett. **25**, 316 (1970) [Erratum-ibid. **25**, 902 (1970)].
[10] L. D. Landau and I. Y. Pomeranchuk, Dokl. Akad. Nauk SSSR **92**, 535 (1953); Dokl. Akad. Nauk SSSR **92**, 735 (1953); English translation in *The Collected Papers of L. D. Landau,* Edited by D. Ter Haar, Pergamon Press, (1965), sections 76, p. 586; A. B. Migdal, Phys. Rev. **103**, 1811 (1956).
[11] J. Raufeisen, J.-C. Peng, and G. C. Nayak, paper in preparation.
[12] V. N. Gribov, Sov. Phys. JETP **29**, 483 (1969) [Zh. Eksp. Teor. Fiz. **56**, 892 (1969)].
[13] V. Karmanov and L. Kondratyuk, JETP Lett. **18**, 266 (1973).
[14] H. I. Miettinen and J. Pumplin, Phys. Rev. D **18**, 1696 (1978).
[15] N. N. Nikolaev and B. G. Zakharov, Z. Phys. C **49**, 607 (1991).
[16] J. Raufeisen, Ph.D. thesis, Heidelberg, 2000, hep-ph/0009358.
[17] B. Z. Kopeliovich, J. Raufeisen and A. V. Tarasov, Phys. Rev. C **62**, 035204 (2000)
[18] B. Z. Kopeliovich, J. Raufeisen and A. V. Tarasov, Phys. Lett. B **440**, 151 (1998) J. Raufeisen, A. V. Tarasov and O. O. Voskresenskaya, Eur. Phys. J. A **5**, 173 (1999)
[19] B. Z. Kopeliovich, A. Schäfer and A. V. Tarasov, Phys. Rev. D **62**, 054022 (2000)
[20] B. Z. Kopeliovich, J. Raufeisen and A. V. Tarasov, Phys. Lett. B **503**, 91 (2001)
[21] B. Z. Kopeliovich, J. Raufeisen and A. V. Tarasov, arXiv:hep-ph/0104155.
[22] K. Golec-Biernat and M. Wüsthoff, Phys. Rev. D **59**, 014017 (1999); Phys. Rev. D **60**, 114023 (1999).
[23] M. B. Johnson, *et al.* [FNAL E772 Collab.], *Phys. Rev. Lett.* **86**, 4483 (2001) M. B. Johnson, *et al.*, *Phys. Rev. C* **65**, 025203 (2002) J. M. Moss, *et al.*, arXiv:hep-ex/0109014.
[24] B. Z. Kopeliovich, J. Raufeisen, A. V. Tarasov and M. B. Johnson, arXiv:hep-ph/0110221.
[25] B. Z. Kopeliovich, J. Nemchik, A. Schäfer and A. V. Tarasov, arXiv:hep-ph/0201010.
[26] B. Z. Kopeliovich, J. Nemchik, A. Schäfer and A. V. Tarasov, Phys. Rev. C **65**, 035201 (2002) Y. P. Ivanov, B. Z. Kopeliovich, A. V. Tarasov and J. Hüfner, arXiv:hep-ph/0202216; J. Hüfner, Y. P. Ivanov, B. Z. Kopeliovich and A. V. Tarasov, Phys. Rev. D **62**, 094022 (2000)